Nuclear reactions of silver with 11.5-GeV protons*

G. English and N. T. Porile
Department of Chemistry, Purdue University, Lafayette, Indiana 47907
E. P. Steinberg
Chemistry Division, Argonne National Laboratory, Argonne, Illinois 60439
(Received 24 June 1974)

The interaction of silver with 11.5-GeV protons was studied and formation cross sections of 72 radionuclides were determined by direct assay of the target with a Ge(Li) γ-ray spectrometer followed by computer analysis of the spectra. The data were used to construct charge-dispersion and mass-yield curves. Comparison with previous radiochemical studies performed with 29-GeV protons indicates good agreement between the two techniques. The data are compared with Rudstam systematics. This formulation predicts a much steeper decrease in isobaric cross sections with decreasing A than is observed experimentally.

[NUCLEAR REACTIONS Ag + 11.5-GeV protons; measured σ for formation of 72 nuclides ranging from ^{7}Be to ^{106}Ag^{m}; deduced charge dispersions and mass yield curve.]

I. INTRODUCTION

The recent availability of 300-GeV proton beams at the National Accelerator Laboratory has made it of interest to extend studies of the interaction of high-energy protons with complex nuclei into this new energy range. In order to obtain the most meaningful results on possible energy-dependent changes in the nature of the interaction it is necessary to perform comparative studies using insofar as possible the same techniques. We report here the results of a study of the nuclear reactions induced in silver by 11.5-GeV protons performed in order to permit a comparison with similar data obtained at 300 GeV.[1,2]

A convenient technique for the simultaneous determination of a large number of cross sections is the direct assay of an irradiated target foil with a lithium-drifted germanium detector followed by subsequent computer analysis of the γ-ray spectra. This technique has been employed in a number of high-energy nuclear reaction studies.[3-10] Although the method appears to be most reliable for low-Z targets, where the number of radioactive products formed is relatively small, it has been successfully used on target elements as heavy as uranium.[4] The extensive study of reactions of silver with 3- and 29-GeV protons performed by Katcoff, Fickel, and Wyttenbach[11] using conventional radiochemical techniques makes a large number of cross sections available for comparison with the present work and thus serves as a check on the direct assay technique.

II. EXPERIMENTAL

The irradiations were performed in the internal circulating beam of the zero gradient synchrotron (ZGS) at Argonne National Laboratory. The results are based on seven irradiations whose duration ranged from a few seconds (1 or 2 pulses) to 20 minutes.

The target stacks consisted of two 20 μm aluminum foils and three 25 μm silver foils wrapped with 20 μm aluminum. Both materials were of high purity (>99.99%). The foils were carefully aligned to insure that they intercepted the same number of protons and the stack was mounted on a target holder with the aluminum foils on the upstream side. The middle foil of each material was used for analysis while the outer foils served to compensate for recoil loss and to prevent cross contamination.

Following the irradiations the target foil was directly assayed with a Ge(Li) γ-ray spectrometer. Measurements on short-lived nuclides were performed at Argonne and commenced about 8 min after the end of bombardment. The Argonne system consisted of a detector with an efficiency of 6% (relative to NaI) and a resolution of 2.0 keV (at 1332.5 keV). The detector was connected to a 4096-channel analyzer equipped with magnetic tape readout. Measurements on products having half-lives longer than 4 hours were performed at Purdue. Assay commenced from 3 h to 2 days after bombardment, depending on the half-lives of interest, and continued for as long as 1.5 yr. The Purdue system consisted of a detector with an efficiency of 4.5% and a resolution of 2.7 keV, connected to a 4096-channel analyzer equipped with punched paper tape readout. Towards the end of the experiment a detector with a resolution of 1.9 keV became available and some comparative measurements were made.

The aluminum monitor foils were also assayed with the above-mentioned Ge(Li) detectors in order to determine the disintegration rate of ^{24}Na

formed by the $^{27}Al(p, 3pn)$ monitor reaction. Cross sections were determined relative to the 8.6 mb cross section[12] of the monitor reaction.

The various Ge(Li) detectors were calibrated with carefully standardized sources. The concordance between γ rays from different sources indicates that the uncertainty in absolute efficiency is less than 5%. The various samples were assayed at distances from the face of the detector ranging from 2.5 to 10 cm. It was established that under these conditions corrections due to summing effects were negligible.

The γ-ray spectra were analyzed with a number of codes in order to obtain cross sections. The γ-ray energies and intensities were determined with the BRUTAL program.[13] In this code peaks are found on the basis of a calculation of the direction and statistical significance of the slope at each point in the spectrum followed by Gaussian and statistical tests of each peak-like region. The background under each peak is determined by linear interpolation between the lowest three consecutive points on each side of the peak. Peaks are classified as singlets if they are separated by more than five channels from neighboring peaks. If this is not the case the peaks are considered as being doublets or triplets and the background is obtained by linear interpolation between the lowest points on either side of the group of peaks under consideration. The net number of counts is apportioned between the overlapping peaks in proportion to the net peak heights. In the case of peaks belonging to multiplets, the final peak intensity is chosen as the largest value of the intensities obtained from the singlet, doublet, or triplet analyses.

The presently used version of BRUTAL incorporated the code FRANTIC.[14] This routine determined an approximate half-life for each of the peaks found by BRUTAL in the various spectra from a given bombardment. If necessary, FRANTIC could assign two components to each peak. The combination of energy and half-life determinations permitted nuclidic assignments to be made. The activities of the observed nuclides at the end of bombardment were then obtained with the CLSQ code[15] using the best literature values for the half-lives. The particular version of CLSQ[16] used in this work allowed the separate determination of parent and daughter activities in cases where both members of a genetically related pair of nuclides contributed to an observed peak. Although most γ rays used for cross-section determinations could be assigned to a single nuclide, there were a number of two-, and three-, and even one four-component decay curve analyzed by CLSQ. The cross sections were finally evaluated with an auxiliary program on the basis of the best available γ-ray abundance data. Table I lists the assumed half-lives and abundances, and also identifies decays involving more than one component. A portion of a typical γ-ray spectrum, in this instance a spectrum obtained one day after irradiation, is shown in Fig. 1. Known γ rays are appropriately identified and those used for cross-section determinations are starred.

The reliability of the BRUTAL code was checked by a comparison of calculated peak intensities with hand-integrated values. It was determined that in the case of peaks found to be singlets or dominant components of doublets or triplets the intensities agreed with each other to within approximately 3%. For example, Fig. 1 includes peaks of 484.8 and 559 keV which have been assigned to ^{87}Y and ^{76}Br, respectively. The former is a singlet and the latter the dominant member of a doublet with the 554-keV γ ray due to $^{82}Rb^{m}$. The BRUTAL intensities agree with hand-integrated values within 1 and 5%, respectively. The BRUTAL intensities of peaks that were major components of multiplets agreed with the hand analysis to within about 10%. For instance, in Fig. 1 the 645.5-keV and 656-keV γ rays due to $^{106}Ag^{m}$ and ^{76}Br, respectively, are comparably intense members of a doublet. The intensities obtained by BRUTAL differ from the hand-integrated values by 10 and 15%, respectively. On the other hand, the BRUTAL intensities of minor components of a multiplet were in a number of instances found to be in error by as much as a factor of 2. The 820 keV γ ray assigned in Fig. 1 to ^{100}Rh and ^{100}Pd is a case in point. The BRUTAL intensity of this γ ray, which together with the neighboring peaks at 814 and 833.9 keV comprises a triplet, differs by 27% from the hand-integrated value. Accordingly, peaks that fell in this category were either not used or were integrated by hand. Hand integration was also found to be necessary in the case of moderately weak low-energy singlets or of those lying in the vicinity of the intense 511 keV annihilation peak. Table I identifies all γ rays that required hand-integration.

An additional useful criterion for the validity of the BRUTAL analysis was the quality of the fit of the data for a given peak obtained by the CLSQ code. In a number of instances the BRUTAL peak selection criteria identified a given peak as a singlet in one spectrum, a doublet in another, and perhaps even a triplet in a third. In those cases where the BRUTAL analysis worked well CLSQ was able to fit the decay curve with the appropriate half-life in spite of the variability in peak multiplicity. In some instances, however, many of the data points comprising a given decay curve were found to be inconsistent with the known half-

TABLE I. Decay properties of observed nuclides.

Nuclide	Mode of decay	$t_{1/2}$	Observed γ ray (keV)	Branching ratio
^{7}Be	EC	53.0 day	477.4 [a]	0.103 [b]
^{22}Na	β^+, EC	2.62 yr	1274.6	1.00
^{24}Na	β^-	15.0 h	1368.5 [c]	1.00
^{28}Mg	β^-	21.0 h	1778.5 (^{28}Al) [d]	1.00
^{38}Cl	β^-	37.3 min	1642.7	0.35
			2167.6	0.47
^{41}Ar	β^-	1.83 h	1293.6	0.99
^{44}Sc	β^+, EC	3.92 h	1157.0 [e]	1.00
^{44}Sc^m	86%IT, 14%EC	2.44 day	270.4	0.86
			1157.0 (^{44}Sc)	1.00 [f]
^{46}Sc	β^-	83.9 day	889.2	1.00
			1120.6 [c]	1.00
^{47}Sc	β^-	3.43 day	159.4	0.73 [g]
^{48}Sc	β^-	1.83 day	983.4 [h]	1.00
			1312 [h]	1.00
^{48}V	β^+, EC	16.0 day	983.4 [h]	1.00
			1312 [h]	0.97
^{52}Mn	β^+, EC	5.7 day	744.1	0.88
			935.5 [i]	0.94
			1434.3	1.00
^{52}Mn^m	98%β^+, EC 2%IT	21.3 min	1434.3	0.98
^{54}Mn	EC	303.0 day	834.8 [j]	1.00
^{59}Fe	β^-	45.0 day	1099.3	0.565
			1291.6	0.432
^{56}Co	β^+, EC	77.0 day	1238.3	0.666
			1771.2 [k]	0.162
			2598.5	0.172
^{57}Co	EC	270.0 day	121.9 [l]	0.87
^{58}Co	β^+, EC	71.3 day	810.6	0.99
^{60}Co	β^-	5.26 yr	1173.2	1.00
			1332.5	1.00
^{60}Cu	β^+, EC	23.4 min	1332.5	1.00
^{65}Zn	β^+, EC	245.0 day	1115.4 [c]	0.49
^{66}Ga	β^+, EC	9.4 h	1039.0	0.39
^{67}Ga	EC	78.0 h	184.6	0.24
			300.0	0.16
^{71}As	β^+, EC	62.0 h	174.5 [c]	0.90
^{72}As	β^+, EC	26.0 h	833.9 [j]	1.00
^{74}As	68%β^+, EC 32%β^-	17.9 day	596.0	0.595
			634.9	0.148
^{72}Se	EC	8.4 day	833.9 [j] (^{72}As)	1.00
^{73}Se	β^+, EC	7.1 h	361.1	1.00
^{75}Se	EC	120.4 day	264.6	0.61
^{76}Br	β^+, EC	16.1 h	657.2	0.19
			1216.2	0.13
^{77}Br	β^+, EC	57.0 h	238.9 [c]	0.26
^{79}Rb	β^+, EC	24.0 min	150.0 [c, m]	0.73
^{81}Rb	β^+, EC	4.7 h	190.4 [c]	0.64
^{82}Rb^m	EC	6.4 h	554.3 [n]	0.70
^{83}Rb	EC	83.0 day	520.4 [c]	0.47
			529.6 [c]	0.304
			552.6	0.166
^{84}Rb	97%β^+, EC 3%β^-	33.0 day	881.5	0.734
^{84}Rb^m	≤100%IT, EC (weak)	20.0 min	215.4 [c]	0.37
			247.9 [c]	0.65
^{82}Sr	EC	25.0 day	776.6 [o] (^{82}Rb)	0.134
^{84}Y	β^+, EC	41.0 min	795.0 [p]	1.00

TABLE I *(Continued)*

Nuclide	Mode of decay	$t_{1/2}$	Observed γ ray (keV)	Branching ratio
			974.4 [p]	0.79
$^{86}Y^m$	IT	48.0 min	208.0 [c]	0.94
^{87}Y	β^+, EC	80.0 h	388.3 ($^{87}Sr^m$)	0.80
			484.8	0.92
$^{87}Y^m$	IT	14.0 h	380.7 [q]	0.74
^{88}Y	β^+, EC	108.0 day	1836.1 [r]	1.00
^{86}Zr	EC	16.5 h	243.0 [c]	0.96
^{88}Zr	EC	85.0 day	392.8	0.97
^{89}Zr	β^+, EC	78.4 h	909.2	1.00
^{89}Nb	β^+, EC	1.9 h	587.8 ($^{89}Zr^m$)	1.00
^{90}Nb	β^+, EC	14.6 h	1128.7	0.97
			2318.7	0.82
$^{92}Nb^m$	β^+, EC	10.16 day	934.5	0.975
^{95}Nb	β^-	35.0 day	765.8 [s]	0.99
^{90}Mo	β^+, EC	5.7 h	122.5	0.71
			257.3	0.85
$^{93}Mo^m$	IT	6.9 h	685.0	1.00
			1479.0	1.00
^{94}Tc	β^+, EC	293.0 min	849.7 [t]	1.00
			870.9	1.00
^{95}Tc	EC	20.0 h	765.8 [s]	1.00
$^{95}Tc^m$	β^+, EC [u]	61.0 day	203.9	1.00
			582.2	0.55
^{96}Tc	EC	4.3 day	780.0	1.00
			814.0	0.82
			851.0 [t]	0.99
^{95}Ru	β^+, EC	1.7 h	336.4	0.70
			1097.4	0.21
^{97}Ru	EC	2.9 day	215.2	0.91
			324.2	0.11
^{103}Ru	β^-	39.6 day	497.1	0.90
^{100}Rh	β^+, EC	20.0 h	540.0 [v]	0.88
			2380.0 [v]	0.39
^{101}Rh	EC	3.0 yr	197.9	0.75
$^{101}Rh^m$	93%β^+, EC	4.5 day	309.0 [w]	0.878
	7%IT		548.0 [w]	0.040
^{102}Rh	16%β^-	206.0 day	475.1	0.46
	84%β^+, EC			
$^{102}Rh^m$	EC	2.9 yr	631.4	0.52
^{99}Pd	β^+, EC	22.0 min	136.0	1.00
^{100}Pd	EC	4.0 day	540.0 [v] (^{100}Rh)	0.88
			2380.0 [v] (^{100}Rh)	0.39
^{103}Ag	β^+, EC	66.0 min	118.0 [c]	0.26
			148.0 [c, m]	0.23
^{104}Ag	β^+, EC	67.0 min	556.0	0.84
			767.6 [s]	0.48
$^{104}Ag^m$	β^+, EC	30.0 min	556.0	1.00
^{105}Ag	EC	40.0 day	280.4	0.32
			443.3	0.10
$^{106}Ag^m$	EC	8.4 day	406.0	0.15
			429.5	0.16
			450.8	0.31
			616.0	0.243
			717.1	0.32
			748.2	0.23
			803.9	0.124

TABLE I *(Continued)*

Nuclide	Mode of decay	$t_{1/2}$	Observed γ ray (keV)	Branching ratio
			824.5	0.16
			1045.7	0.28
			1199.1	0.106
			1527.0	0.15

[a] ^{102}Rh (206 day) and ^{102}Rh^m (2.9 yr) both have γ rays in the immediate region of ^{7}Be. The ^{102}Rh^m was determined by its 631.4-keV γ ray. The contribution of this isomer at 476 keV was then subtracted, leaving a two-component decay of ^{7}Be and ^{102}Rh.

[b] Unless otherwise indicated, all branching ratios are from M. A. Wakat, Nucl. Data A 8, 445 (1971), and C. M. Lederer, J. M. Hollander, and I. Perlman, *Table of Isotopes* (Wiley, New York, 1967), 6th ed.

[c] Hand integration required.

[d] Daughter γ ray.

[e] Two-component parent-daughter decay.

[f] L. Husain and S. Katcoff, Phys. Rev. C 7, 2452 (1973).

[g] An 0.3% contribution from ^{101}Rh^m through its 157-keV γ ray is expected based on data by J. Sieniawski, H. Pettersson, and B. Nyman, Z. Phys. 245, 81 (1971).

[h] Two-component decay (^{48}Sc and ^{48}V).

[i] Two-component decay (^{52}Mn and ^{92}Nb^m).

[j] Three-component decay (^{72}As, ^{72}Se, ^{54}Mn).

[k] Listed as 1750 keV in Katcoff, Fickel, and Wyttenbach (Ref. 11).

[l] The contribution from ^{75}Se (121.1 keV) was subtracted.

[m] Two-component decay (^{79}Rb and ^{103}Ag).

[n] Three-component decay (^{104}Ag^m, ^{104}Ag, and ^{82}Rb^m).

[o] Three-component decay (^{82}Rb^m, ^{86}Y, and ^{82}Sr).

[p] Nucl. Data B 5, 125 (1971).

[q] Two-component decay (^{87}Y^m and ^{83}Sr).

[r] Two-component parent-daughter decay (^{88}Y and ^{88}Zr).

[s] Four-component decay (^{104}Ag, ^{95}Nb, ^{95}Tc, and ^{102}Rh^m).

[t] Two-component decay (^{94}Tc and ^{96}Tc).

[u] No isomeric transition seen by G. Chilosi, E. Eichler, and N. K. Aras, Nucl. Phys. A123, 327 (1969).

[v] Two-component parent-daughter decay (^{100}Rh and ^{100}Pd).

[w] J. Sieniawski, H. Pettersson, and B. Nyman, Z. Phys. 245, 81 (1971).

life of the nuclide in question. These γ rays were usually not used for cross-section determinations.

The BRUTAL analysis of the various spectra found a total of 350 distinct γ rays. 65 of these were used for cross-section determinations although, as indicated in Table I, some of them were members of multicomponent decay curves and so were actually different γ rays. The remaining γ rays were not used because either nuclidic assignments could not be made, the abundances were unknown, or the peak intensities could not be obtained in a reliable manner. Whenever possible, cross sections were based on more than one γ ray and if the results were not in accord with each other the data for the nuclide in question were discarded. In spite of these various difficulties it was still possible to determine 72 formation cross sections.

A few comparative measurements were performed with the 2.7-keV resolution detector and one of comparable efficiency having a resolution of 1.9 keV in order to determine the effect of this important variable. In typical measurements performed 10 h after irradiation the BRUTAL analysis found 75 peaks in the spectrum taken with the 2.7-

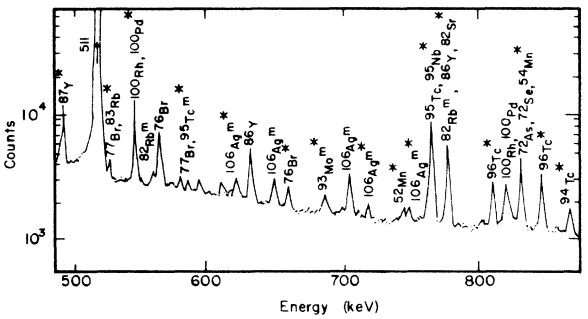

FIG. 1. Portion of a γ-ray spectrum of a silver target recorded ~ 1 day after bombardment. Nuclidic assignments of identified γ rays are indicated; starred peaks were used for cross-section determinations.

keV detector and 102 peaks in that obtained with the 1.9-keV detector. The difference in these numbers was due in approximately equal measure to the following two factors. First, the high-resolution detector yielded a number of weak lines that were unable to meet the statistical significance criteria for acceptability in the spectra taken with the lower-resolution detector. Second, the code found a number of doublets and triplets in the high-resolution spectra that were sufficiently close in energy that they appeared as singlets or doublets, respectively, in the low-resolution spectra. The first of these factors does not affect the accuracy of the data taken with the 2.7-keV detector but would presumably make it possible to determine additional cross sections provided the weak lines could be identified and their abundances were known. On the other hand, the second factor can indeed have a significant effect on the present data since some of the γ rays would have hidden contributions from weaker lines having nearly the same energy. Fortunately, the FRANTIC and CLSQ analyses resolved these γ rays provided they decayed with half-lives that differed by more than a factor of 2. If the half-lives differed between about 40 and 100%, the CLSQ analysis would give a very poor fit to the data on the basis of either a one- or two-component decay, and the data were usually discarded. The only real error occurred in the relatively few cases where the peaks were contaminated by weaker lines decaying with nearly the same half-life. Nonetheless, it is quite clear that the quality and abundance of the data obtainable by this technique are closely related to the resolution of the detector.

III. RESULTS

The cross sections measured in this work are tabulated in Table II. Each yield is identified as being either cumulative (C) or independent (I). The standard deviations quoted for each cross section are based on the agreement between replicate determinations, whose number is listed in column 4. In those instances where more than one γ ray was used for the determination of a particular cross section the results were combined provided they either agreed within their respective uncertainties or differed by less than 10%. If these criteria were not met either separate cross sections based on each γ ray are quoted or the results were discarded, depending on the magnitude of the discrepancy. In addition to the quoted uncertainties, which are a measure of random errors, the cross sections suffer from systematic errors in detector efficiency (±5%), γ-ray abundance (±0–15%), and the cross section of the monitor reaction (±7%). The cross sections were not corrected for possible contributions of secondary reactions to either the monitor or the target activities. Previous studies[17] have indicated that such corrections should be small (<2%) for the target assemblies used in this work.

Katcoff *et al.*[11] measured the cross sections of some 60 nuclides formed in the interaction of silver with 3- and 29-GeV protons. Their cross-section tabulation includes some additional data, chiefly rare-gas yields.[18] In view of the fact that these workers report significant differences between the yields determined at these two energies while, as shown in the accompanying report,[2] there appears to be little if any difference between the 11.5- and 300-GeV results, it is most appropriate to compare the present data with the 29-GeV values. The cross sections obtained at 29 GeV are tabulated in column 5 of Table II while the ratios $\sigma_{29}/\sigma_{11.5}$ are listed in the last column. In general, the agreement between the two sets of data is gratifyingly good. The main discrepancy occurs for ^{79}Rb whose cross sections differ by over a factor 2. The cross section quoted by Katcoff *et al.*[11] actually comes from an unpublished private communication and appears to be anomalous because the value of σ_{29}/σ_3 is 4 (Ref. 11), which is far larger than any of the other reported ratios. Excluding the result for this nuclide the values of $\sigma_{29}/\sigma_{11.5}$ agree, on the average, to within 15%, a value that is well within the estimated uncertainties in the ratios. Moreover, there appear to be no systematic differences between the two sets of data. This comparison thus serves to confirm the validity of the present approach to cross-section determinations.

A preliminary tabulation of some of the presently reported cross sections appeared in an earlier report.[1] Some of these preliminary values are incorrect. The largest discrepancies occur for ^{74}As, misprinted as 5.9 mb; ^{83}Rb, for which hand-integration was necessary but had not been performed; and ^{7}Be, whose 477 keV γ ray included an unresolved contribution from long-lived ^{102}Rh.

IV. DISCUSSION

A. Determination of charge dispersion

The present data are sufficiently complete to permit a fairly detailed determination of the charge-dispersion and mass-yield curves. Separate charge dispersions were determined for nine mass intervals spanning the $A = 22-106$ region. Preliminary curves were drawn through independent yields as well as cumulative yields that

TABLE II. Product cross sections from bombardment of silver with 11.5-GeV protons and comparison with previous data at 29 GeV.

Nuclide	Type of yield	$\sigma_{11.5}$ (mb)	No. of det.	σ_{29} [a] (mb)	$\sigma_{29}/\sigma_{11.5}$
^{7}Be	C	14.2 ± 1.0 [b]	2 [c]	18.2 [d]	1.28
^{22}Na	C	1.6 ± 0.1	2	2.35 [e]	1.47
^{24}Na	C	3.9 ± 0.4	2	4.10	1.05
^{28}Mg	C	0.60 ± 0.01	2	0.594	0.99
^{38}Cl	I [f]	1.2 ± 0.1	2	...	
^{41}Ar	C	0.65 ± 0.03	2	0.63 [g]	0.97
^{44}Sc	I	1.44 ± 0.04	2	1.12	0.78
^{44}Sc^{m}	I	1.9 ± 0.1	2	2.06 [h,i]	1.08
^{46}Sc	I	3.0 ± 0.4	3	3.44	1.15
^{47}Sc	I [j]	2.08 ± 0.01	2	1.63 [i]	0.78
^{48}Sc	I	0.55 ± 0.08	2 [k]	0.47 [l]	0.85
^{48}V	C	2.5 ± 0.2	3 [m]	2.81 [i,n]	1.12
^{52}Mn	I [o]	1.7 ± 0.1	3 [p]	...	
^{52}Mn^{m}	I [q]	0.39 ± 0.05	3	...	
^{54}Mn	I	4.8 ± 0.2	2	5.55	1.16
^{59}Fe	C	0.60 ± 0.04	3	0.626 [r]	1.04
^{56}Co	C	1.5 ± 0.2	3 [s]	~1.9 [i]	1.27
^{57}Co	C	4.4 ± 0.7	2	4.31 [t]	0.98
^{58}Co	I	5.8 ± 0.6	3	5.51 [u]	0.95
^{60}Co	I	1.90 ± 0.04 [v]	2	2.05 [w]	1.08
		1.6 ± 0.1 [x]	2		
^{60}Cu	C	0.70 ± 0.03	2	...	
^{65}Zn	C	8.8 ± 0.3	2	8.89 [i]	1.01
^{66}Ga	C	4.3 ± 0.1	2	...	
^{67}Ga	C	7.6 ± 0.4 [y]	2	7.31 [i,z]	0.96
		10.9 ± 0.1 [aa]	2		
^{71}As	C	7.0 ± 0.2	2	6.39 [i]	0.91
^{72}As	I	5.9 ± 0.3	2	5.13 [i]	0.87
^{74}As	I	1.8 ± 0.2 [bb]	3	2.49 [i,cc]	0.92
		2.7 ± 0.3 [dd]	3		
^{72}Se	C	2.2 ± 0.1	2	1.90 [i]	0.86
^{73}Se	C	3.8 ± 0.3	3	...	
^{75}Se	C	9.8 ± 0.5	2	12.1 [i,ee]	1.23
^{76}Br	I [ff]	8.1 ± 0.2	2	...	
^{77}Br	C	8.9 ± 0.6	2	...	
^{79}Rb	C [gg]	2.0 ± 0.3	3	4.6	2.30
^{81}Rb	C	16.0 ± 1.3	2	...	
^{82}Rb^{m}	I	4.8 ± 0.1	2	...	
^{83}Rb	C	12.3 ± 0.4	3	14.9 [i]	1.21
^{84}Rb	I	1.31 ± 0.02	3	1.53 [i]	1.17
^{84}Rb^{m}	I	0.71 ± 0.02 [hh]	2	...	
		0.89 ± 0.02 [ii]	2		
^{82}Sr	C	7.1 ± 0.5	4	6.36 [jj]	0.90
^{84}Y	I [kk]	4.5 ± 0.7	3	...	
^{86}Y^{m}	I	5.8 ± 0.2	3	...	
^{87}Y	C	17.6 ± 0.7	2	...	
^{87}Y^{m}	C	15.0 ± 1.3	3	...	
^{88}Y	I	3.9 ± 0.2	2	...	
^{86}Zr	C	5.0 ± 0.3	3	...	
^{88}Zr	C	14.6 ± 1.2	4	15.4 [i]	1.05
^{89}Zr	C	15.7 ± 0.9	5	17.5	1.11
^{89}Nb	C	1.6 ± 0.2	4	...	
^{90}Nb	C	16.0 ± 1.2	3	...	
^{92}Nb^{m}	I	0.64 ± 0.05	2	...	
^{95}Nb	I [ll]	0.43 ± 0.04	3	...	
^{90}Mo	C	3.3 ± 0.6	2	...	
^{93}Mo^{m}	I	3.9 ± 0.8	3	...	
^{94}Tc	C	6.62 ± 0.01 [mm]	2	...	
		7.8 ± 0.2 [nn]	2		
^{95}Tc	C [oo]	15.7 ± 1.3	3	...	
^{95}Tc^{m}	I	0.75 ± 0.1	2	...	
^{96}Tc	I	7.1 ± 0.5	4 [pp]	...	
^{95}Ru	C	5.7 ± 0.7	3	...	
^{97}Ru	C	14.2 ± 1.0	2 [qq]	18.5 [i,rr]	1.30
^{103}Ru	C	1.26 ± 0.01	2	0.90 [i]	0.71
^{100}Rh	I	11.1 ± 0.7	3 [ss]	...	
^{101}Rh	I [tt]	3.8 ± 0.1	2	3.47 [i]	0.91
^{101}Rh^{m} [uu]	C	18.6 ± 1.3	2 [vv]	...	
^{102}Rh	I	1.2 ± 0.3	2	...	
^{102}Rh^{m}	I	4.5 ± 0.3	2	...	
^{99}Pd	C	1.64 ± 0.01	3	...	
^{100}Pd	C	4.3 ± 0.3 [ww]	5	5.63 [xx]	1.31
		5.2 ± 0.1 [yy]	3		
^{103}Ag	C	7.7 ± 0.5 [zz]	2	8.08 [aaa]	1.05
		12.4 ± 0.4 [bbb]	3		
^{104}Ag	I [ccc]	9.4 ± 1.0	2	...	
^{104}Ag^{m}	C [ddd]	5.0 ± 0.6	2	...	
^{105}Ag	C	25.0 ± 1.7	2 [eee]	28.4 [fff]	1.14
^{106}Ag^{m}	I	9.4 ± 0.7	4 [ggg]	...	

[a] Reference 11.

[b] Only random uncertainties are listed; see text for magnitude of systematic errors.

[c] Number of bombardments in which nuclide was observed; if more than one γ ray was used for cross section determinations the total number of determinations is correspondingly larger.

[d] J. Hudis (private communication), method of determination unknown.

[e] Based on the 511- and 1274.6-keV γ rays.

[f] The ^{38}S ($t_{1/2}$ = 2.87 h) parent contributes in part to the ^{38}Cl counting rate but the charge dispersion indicates that its cross section is <0.1 mb.

[g] I. Dostrovsky and R. W. Stoenner (private communication), mass spectrometric determination.

[h] Based only on the 270.4-keV γ ray.

[i] σ corrected to agree with present γ-ray abundances.

[j] The ^{47}Ca($t_{1/2}$ = 4.5 day) parent contributes in part to the ^{47}Sc counting rate but Katcoff *et al.* (Ref. 11) report that its cross section is only 0.09 mb.

[k] Two determinations for the 983.4-and three determinations for the 1312.1-keV γ ray.

[l] Based on the 1312.1-keV γ ray only.

TABLE II *(Continued)*

[m] Three determinations for the 983.5-and four determinations for the 1311.9-keV γ ray.
[n] Based on the 1311.9-keV γ ray only.
[o] Includes 2% of the $^{52}Mn^{m}$ yield.
[p] Three determinations for 744.1- and four each for the 935.5- and 1434.3-keV γ ray.
[q] ^{52}Fe(8.2 h) decays to $^{52}Mn^{m}$ but during the time $^{52}Mn^{m}$ was observed in the spectra the contribution of ^{52}Fe was <0.01%.
[r] Based on the 270- and 460-keV β^{-} rays.
[s] Three determinations for the 1238.3- and 2598.5-, and two determinations for the 1771.3-keV γ ray.
[t] Based on 121.9- and 136.3-keV γ rays.
[u] Based on a sum of γ rays between 805 and 845 keV.
[v] Based on the 1173.2-keV γ ray only.
[w] Based on 1173.2- and 1332.5-keV γ rays.
[x] Based on the 1332.5-keV γ ray only.
[y] Based on the 184.6-keV γ ray only.
[z] Based on 184.6- and 209.0-keV γ rays; abundance of 209 assumed to be 0.025.
[aa] Based on the 300.0-keV γ ray only.
[bb] Based on the 596.0-keV γ ray only.
[cc] Based on 596.0- and 634.9-keV γ rays.
[dd] Based on the 634.9-keV γ ray only.
[ee] Based on 265.0- and 280.0-keV γ rays; abundance of the 280 assumed to be 0.25.
[ff] The $^{76}Kr(t_{1/2}=14.8$ h) parent contributes in part to the ^{76}Br counting rate but Katcoff *et al.* (Ref. 11) report that its cross section is only 1.4 mb.
[gg] The half-life of the immediate precursor is unknown.
[hh] Based on the 215.4-keV γ ray only.
[ii] Based on the 247.9-keV γ ray only.
[jj] Based on 511-keV annihilation radiation of ^{82}Rb.
[kk] The $^{84}Zr(t_{1/2}=16$ min) parent contributes in part to the ^{84}Y counting rate but the charge dispersion indicates that its cross section is only 0.3 mb.
[ll] The $^{95}Zr(t_{1/2}=65$ day) parent contributes in part to the ^{95}Nb counting rate but the charge dispersion indicates that its cross section is <0.1 mb.
[mm] Based on the 849.7-keV γ ray only.
[nn] Based on the 870.9-keV γ ray only.
[oo] $^{95}Tc^{m}$ does not decay by IT [G. Chilosi, E. Eichler, and N. K. Aras, Nucl. Phys. A123, 327 (1969)].
[pp] Three determinations for the 780.0-keV γ ray.
[qq] Three determinations for the 324.2-keV γ ray.
[rr] Based on the 215.4-keV γ ray only; however, Katcoff *et al.* (Ref. 11) call the energy 220 keV.
[ss] Four determinations for the 540-keV γ ray.
[tt] This yield contains a 7.2% contribution from $^{101}Rh^{m}$, as determined by J. Sieniawski, H. Pettersson, and B. Nyman, Z. Phys. 245, 81 (1971).
[uu] The total yield of ^{101}Rh (including isomer) is [3.8 mb-(7.2%×18.6 mb)] + 18.6 mb.
[vv] Three determinations for the 548-keV γ ray.
[ww] Based on the 540-keV γ ray only.
[xx] Based on the 19-keV x ray.
[yy] Based on the 2380-keV γ ray only.
[zz] Based on the 118-keV γ ray only.
[aaa] Based on the 20-keV x ray of ^{103}Pd.
[bbb] Based on the 148-keV γ ray only.
[ccc] A discrepancy appears in the literature concerning the occurrence of an isomeric transition in the decay of $^{104}Ag^{m}$. Girgis *et al.* [R. K. Girgis and R. Van Lieshout, Nucl. Phys. 13, 493 (1959)] find no evidence for IT. Ames *et al.* [O. Ames, A. M. Bernstein, M. H. Brennan, R. A. Haberstroh, and D. R. Hamilton, Phys. Rev. 118, 1599 (1960)] report the occurrence of IT in 20–40% of the decays. The present results are based on the assumption of no IT.
[ddd] ^{104}Cd(57 min) decays to $^{104}Ag^{m}$ but no evidence of a 57 min component was seen in the decay curve indicating that the yield of ^{104}Cd is much smaller than that of $^{104}Ag^{m}$.
[eee] Three determinations for the 443.3-keV γ ray.
[fff] Based on the 21-keV x ray.
[ggg] The number of determinations for each γ ray is given in parentheses: 616.0 (2), 803.9 (3), 824.5 (2), 1045.7 (5), 1199.1 (5), 1527.0 (2).

were judged to be mostly independent. The latter were corrected for precursor contribution on the basis of the shapes of the preliminary curves and the results were plotted to give a second approximation to the charge dispersion. The resulting curves were used to obtain a preliminary mass-yield curve and the charge dispersions were further refined by applying a correction for the variation of isobaric yield with A over each mass interval. The final curves obtained in this fashion are

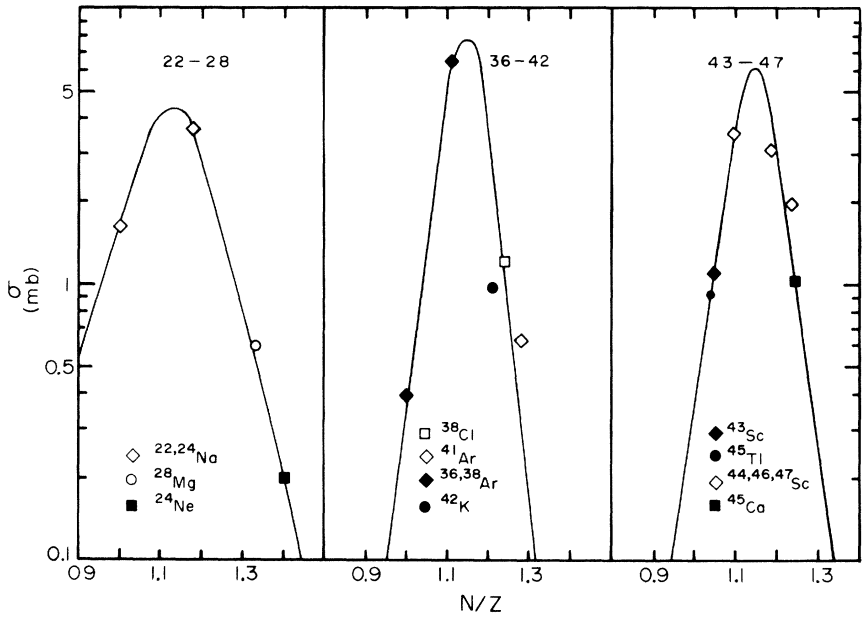

FIG. 2. Charge-dispersion curves for the indicated mass intervals. The cross sections used to construct these curves are shown. Open points are from present work and closed points from Ref. 11.

displayed in Figs. 2–4. In view of the good agreement between the present cross sections and those of Katcoff *et al.*[11] we included some of their 29-GeV data. The curves drawn through the points are merely intended to indicate the trends in the data and are not the result of a fitting procedure. However, they appear to be nearly Gaussian in shape.

The parameters characterizing the charge dispersions are summarized in Table III. The listed quantities are the median mass number for each interval, A_m; the neutron-to-proton ratio at the

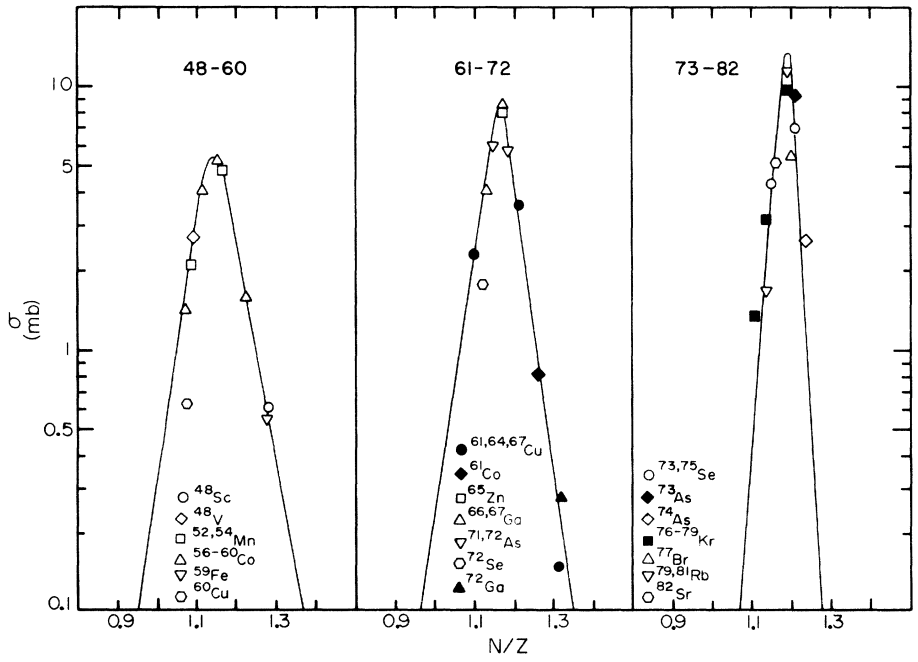

FIG. 3. Charge-dispersion curves for the indicated mass intervals. See Fig. 2 for details.

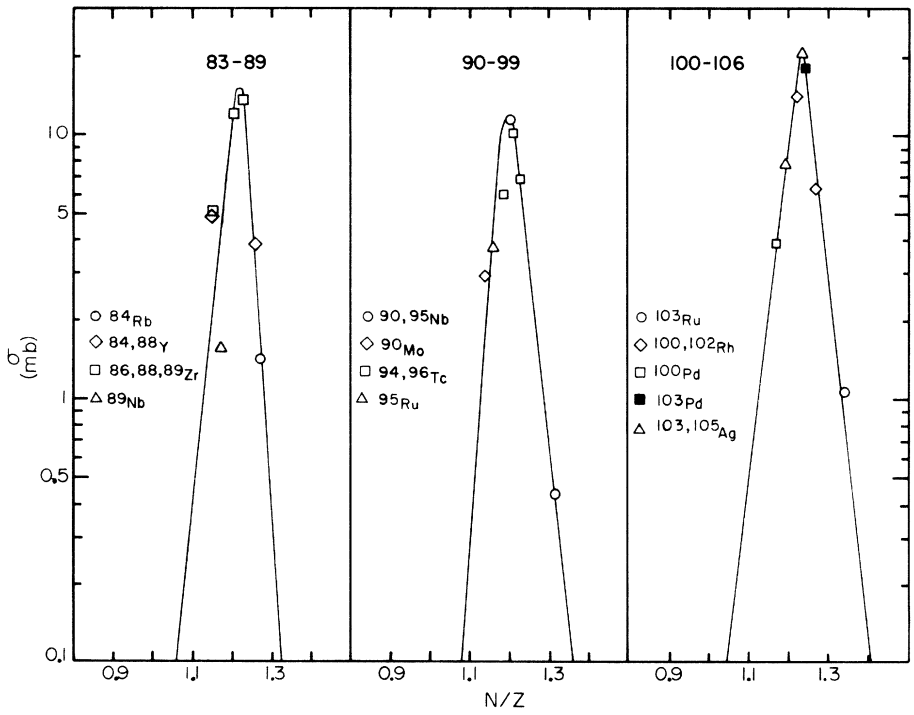

FIG. 4. Charge-dispersion curves for the indicated mass intervals. See Fig. 2 for details.

peaks of the curves, N/Z_p; the corresponding values of the most probable charge evaluated at A_m, Z_p; the full width at half-maximum of the distribution $\Delta(N/Z)$ and the corresponding spread in Z evaluated at A_m, ΔZ; the most stable nuclear charge at A_m, Z_A[19]; and the difference between the most stable and the most probable charge, $Z_A - Z_p$. The most interesting trend is that in the values of $Z_A - Z_p$. It is seen that in the low-mass region, $A < 50$, the peak in the charge dispersion essentially occurs at stability. As A increases the peak position gradually shifts to the neutron deficient side of stability, leveling off at $A \sim 70$ somewhat more than one charge unit beyond the most stable charge.

This trend can be correlated in an approximate way with the transition between spallation and a two-body breakup mechanism. Katcoff *et al.*[11] compared their 3-GeV mass-yield curve with a cascade-evaporation calculation and found that the predicted yields below $A \sim 50$ were very much smaller than the experimental ones, indicating that these products had to be formed by another process, presumably involving two-body breakup. Cumming *et al.*[20] measured the differential ranges of products from the interaction of silver with 2.9-GeV protons. They found that the ranges of products having $A > 42$ were in accord with the results of a cascade-evaporation calculation while that of ^{24}Na indicated the occurrence of two-body breakup. The charge dispersion trend noted above is consistent with this difference in mechanisms.

Katcoff *et al.*[11] performed a similar charge dispersion analysis based on their 3- and 29-GeV data. Their parameters are comparable to the present values which is not surprising in view of the agreement between the experimental cross sections.

B. Mass-yield curve

The charge-dispersion curves were used to construct a mass-yield curve. The total isobaric

TABLE III. Charge dispersion parameters; the various quantities are defined in the text.

Mass region	A_m	N/Z_p [a]	Z_p [b]	$\Delta(N/Z)$ [c]	ΔZ [d]	Z_A	$Z_A - Z_p$ [d]
22–28	24	1.13	11.3	0.22	1.2	11.6	0.3
36–42	38	1.14	17.8	0.11	0.9	17.6	−0.2
43–47	46	1.15	21.4	0.13	1.3	21.2	−0.2
48–60	54	1.14	25.2	0.10	1.4	24.7	−0.4
61–72	66	1.16	30.6	0.06	1.0	29.5	−1.1
73–82	79	1.19	36.1	0.05	0.8	34.6	−1.5
83–89	86	1.22	38.7	0.06	0.9	37.6	−1.1
90–99	95	1.20	43.2	0.08	1.5	41.6	−1.6
100–106	103	1.23	46.1	0.04	0.9	45.1	−1.0

[a] The uncertainty in N/Z_p is ±0.02.
[b] The uncertainty in Z_p is ±1%.
[c] The uncertainty in $\Delta(N/Z)$ is ±0.02.
[d] The uncertainty in ΔZ and in $Z_A - Z_p$ is ±0.2.

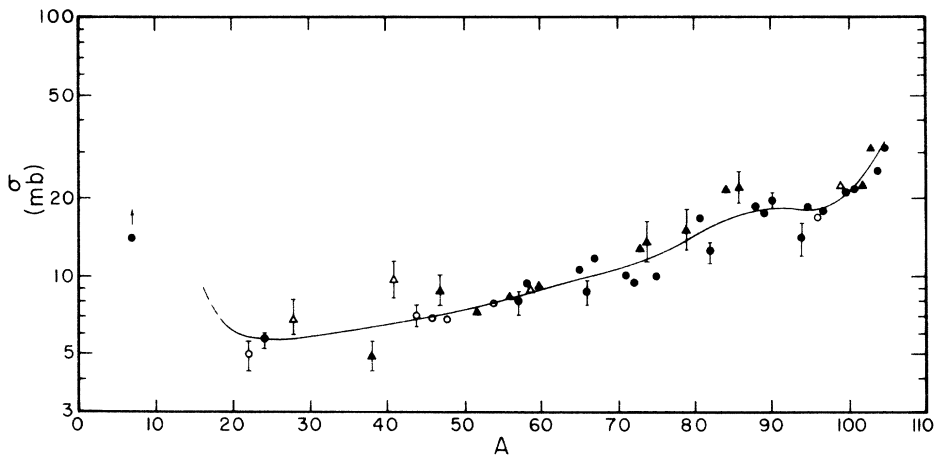

FIG. 5. Mass-yield curve for interaction of Ag with 11.5-GeV protons. The various symbols refer to the fractions of the total isobaric yields that were experimentally determined: ●(> 50%), ○(30–50%), ▲(10–30%), △(< 10%). Typical uncertainties are shown. The solid curve shows the trend of the data and the dashed curve is an extrapolation to lower masses.

yield at each mass number for which a cross section had been measured was obtained by adding the missing isobaric yields to the values listed in Table II. These values were obtained from the charge-dispersion curve appropriate to the mass number in question. The resulting mass-yield curve is displayed in Fig. 5. The various symbols indicate the fractions of the total isobaric cross sections that were experimentally determined. The isobaric cross sections decrease with decreasing A from ~30 mb near the target to a broad minimum of ~6 mb at $A \sim 20$–40 and presumably increase again at lower mass numbers. This upturn is most clearly documented by the counter-telescope data of Hyde, Butler, and Poskanzer.[21] The plateau observed at $A \sim 85$–95 appears to be a real feature but more careful measurements would be needed to establish its existence beyond question.

The mass-yield curve is compared with the corresponding curves derived from the 3- and 29-GeV data (Ref. 11) in Fig. 6. Very good agreement with the 29-GeV curve is obtained over most of the mass range. However, there appear to be significant differences at both the lowest and the highest mass numbers where it can be seen that the present isobaric cross sections are substantially smaller. The discrepancy at $A = 20$–30, which becomes as large as 75%, occurs in spite of the fact that, as seen in Table II, the experi-

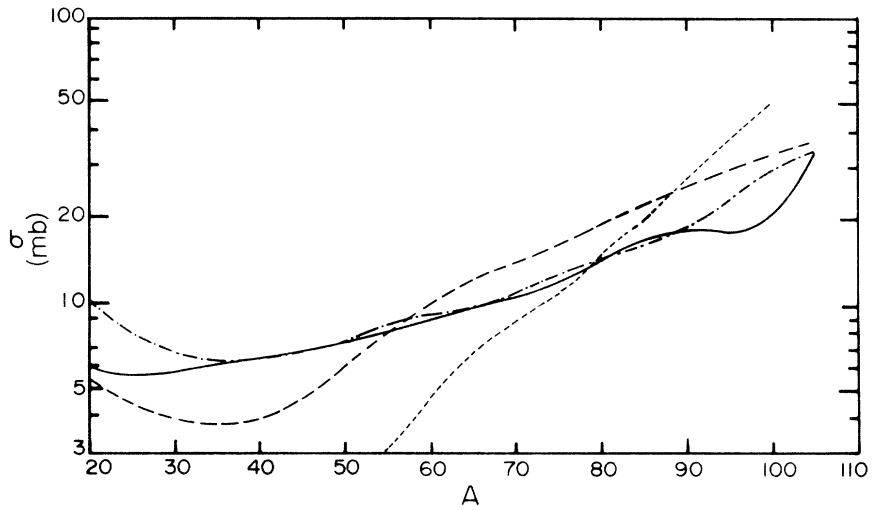

FIG. 6. Comparison of the mass-yield curve at 11.5 GeV (solid line) with that obtained by Katcoff *et al.* (11) at 3 GeV (long-dashed) and at 29 GeV (dot-dashed). The short-dashed curve is from Rudstam systematics.

mental cross sections determined in both studies are in fairly good agreement. Katcoff *et al.*,[11] however, based their total isobaric yields in this mass region on the reported cumulative yields of stable neon isotopes[18] which are much larger than the values based on their charge dispersion. It should be noted that the charge dispersion in this mass region is not very well defined because of the scarcity of measurable yields. The discrepancy between the two studies can thus be attributed to a difference between the mass-spectrometric determinations on the one hand and those based on yields measured either radiochemically or by direct assay combined with those derived from the charge dispersions on the other.

The discrepancy noted in the $A \sim 90-105$ mass region, which is never larger than ~50%, is probably more apparent than real because of the paucity of 29-GeV data. Total isobaric yields in this mass interval are thus only reported at $A = 97$, 101, 103, and 105. On the other hand the present curve is based on points at these four mass numbers plus nine additional ones. The only actual discrepancies occur at $A = 97$ and 101 where the 29-GeV total chain yields are substantially larger than the present values. This difference arises chiefly from that in values estimated from the charge dispersions. Because of the relatively small number of data points in this mass region Katcoff *et al.*[11] used a wider mass interval to construct their charge dispersion than we did and this appears to account for the difference.

The total reaction cross section of silver can be obtained by an appropriate summation of the isobaric yields. If we assume that all products of $A \leq 25$ have higher-mass partners and that none of $A > 25$ do, we can obtain σ_R by addition of all isobaric cross sections for $A > 25$. The result is 1.08 ± 0.16 b, in good agreement with the value of 1.16 ± 0.15 b obtained[11] at 29 GeV. The total reaction cross sections of complex nuclei for 24-GeV protons have been determined by absorption measurements.[22] The results for nuclei above copper obey the relation $\sigma_R = \pi[r_0 A^{1/3}]^2$ with $r_0 = 1.26$ fm. This corresponds to $\sigma_R = 1.13$ b for silver, in excellent agreement with the present determination.

C. Comparison with Rudstam systematics

The results of this study may be compared with the spallation cross-section formula developed by Rudstam.[23] The mass-yield curve predicted by Rudstam's CDMD equation is shown in Fig. 6. The over-all magnitude of the cross sections was ad-

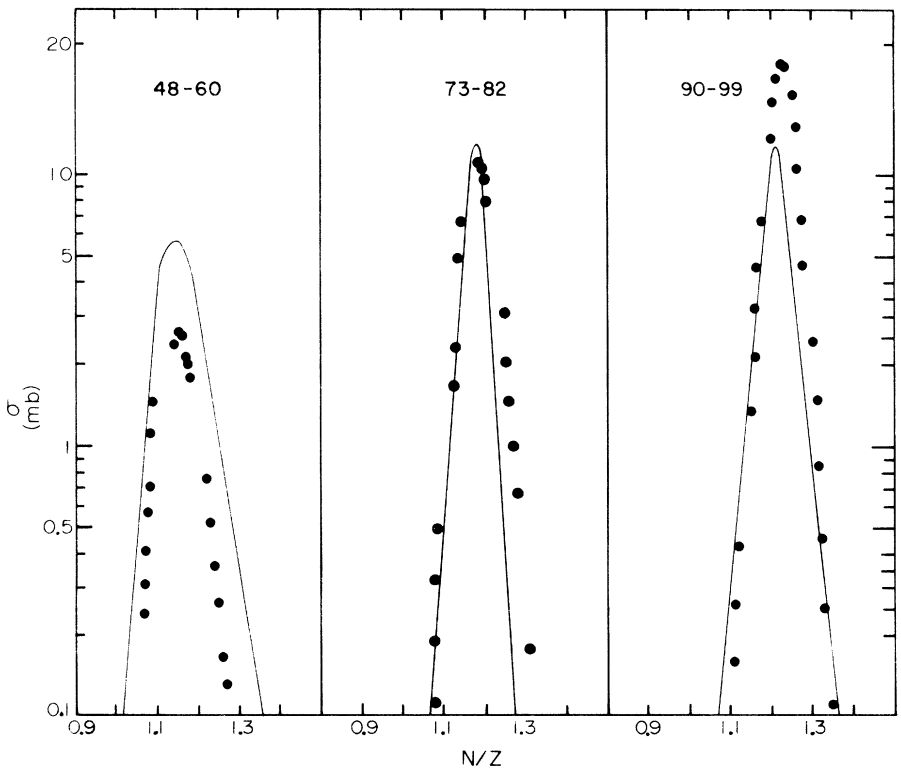

FIG. 7. Comparison of charge dispersions with Rudstam systematics. The solid curves are experimental and the points are from the systematics.

justed by setting the quantity $\hat{\sigma}$ equal to $1.15\sigma_i$, where σ_i is the absorption cross section of silver.[23] This value of $\hat{\sigma}$ gives better agreement with the data than the value $\hat{\sigma} = 1.73\sigma_i$ predicted by the systematics.[23] Even with this adjustment the Rudstam formula gives a very poor fit to the mass-yield curve. The decrease of the calculated isobaric yields thus is much steeper than that of the experimental values. The same conclusion applies to the mass-yield curve calculated by means of the CDMD-G formula.[23]

The calculated and experimental charge dispersions for some of the mass intervals of interest are compared in Fig. 7. The systematics lead to peak positions and widths that are in good agreement with experiment, at least for the lower mass intervals. In the $A \sim 95$ region the calculated curve peaks at a somewhat larger N/Z value and is slightly narrower than the experimental one. These discrepancies are minor compared to that between the peak heights which, of course, is closely related to that between the mass-yield curves.

V. CONCLUSIONS

The technique of gross γ-ray Ge(Li) spectrometry coupled with computer analysis of the spectra has been successfully applied to a study of the nuclear reactions of silver with 11.5-GeV protons. The measurement of 72 formation cross sections permitted the determination of charge-dispersion curves for various mass intervals and led, in turn, to the construction of a mass-yield curve. The peak of the charge dispersion lies at stability for $A < 50$ but shifts to the neutron deficient side at higher mass numbers. The total isobaric yield decreases from about 30 mb close to the target to ~6 mb at $A \sim 20$–40 and appears to increase again at lower mass numbers. These changes appear to be correlated with a transition between spallation and two-body breakup.

The present results are in very good agreement with previous studies[11] of the interaction of silver with 29-GeV protons performed by conventional radiochemical measurements. The results were also compared with Rudstam's spallation systematics.[23] The latter predicts a much steeper mass-yield curve than is observed experimentally.

ACKNOWLEDGMENTS

We wish to thank Dr. Y. W. Yu for valuable discussions and for his help with some of the measurements, Dr. S. Kaufman for his assistance at Argonne National Laboratory, and Dr. S. Katcoff for his advice. The cooperation of the operating staff at the ZGS is appreciated.

---

*Work supported by the U.S. Atomic Energy Commission.

[1]G. English, Y. W. Yu, and N. T. Porile, Phys. Rev. Lett. 31, 244 (1973).

[2]G. English, Y. W. Yu, and N. T. Porile, following paper, Phys. Rev. C 10, 2281 (1974).

[3]I. R. Williams, C. B. Fulmer, G. F. Dell, and M. J. Engebretson, Phys. Lett. 26B, 140 (1968).

[4]B. Schröder, G. Nydahl, and B. Forkman, Nucl. Phys. A143, 449 (1970).

[5]R. L. Brodzinski, L. A. Rancitelli, J. A. Cooper, and N. A. Wogman, Phys. Rev. C 4, 1250, 1257 (1971).

[6]G. J. Kumbartzki, U. Kim, and C. K. Kwan, Nucl. Phys. A160, 237 (1971).

[7]J. E. Cline and E. B. Nieschmidt, Nucl. Phys. A169, 437 (1971).

[8]G. Andersson, I. Blomqvist, B. Forkman, G. G. Jonsson, A. Järund, I. Kroon, K. Lindgren, and B. Schrøder, Nucl. Phys. A197, 44 (1972).

[9]L. Husain and S. Katcoff, Phys. Rev. C 7, 2452 (1973).

[10]S. Katcoff, S. B. Kaufman, E. P. Steinberg, M. W. Weisfield, and B. D. Wilkins, Phys. Rev. Lett. 30, 1221 (1973).

[11]S. Katcoff, H. R. Fickel, and A. Wyttenbach, Phys. Rev. 166, 1147 (1968).

[12]J. B. Cumming, Annu. Rev. Nucl. Sci. 13, 261 (1963).

[13]R. Gunnink, H. B. Levy, and J. B. Niday, University of California Radiation Laboratory Report No. UCID-15140 (unpublished); adaptation by B. R. Erdal.

[14]P. C. Rogers, Massachusetts Institute of Technology Report No. 76, 1962 (unpublished).

[15]J. B. Cumming, National Academy of Sciences Report No. NAS-NS-3107, 1962 (unpublished), p. 25.

[16]J. B. Cumming, private communication.

[17]J. R. Grover, Phys. Rev. 126, 1540 (1962).

[18]J. Hudis, T. Kirsten, R. W. Stoenner, and O. A. Schaeffer, Phys. Rev. C 1, 2019 (1970).

[19]C. D. Coryell, Annu. Rev. Nucl. Sci. 2, 305 (1953).

[20]J. B. Cumming, S. Katcoff, N. T. Porile, S. Tanaka, and A. Wyttenbach, Phys. Rev. 134, B1262 (1964).

[21]E. K. Hyde, G. W. Butler, and A. M. Poskanzer, Phys. Rev. C 4, 1759 (1971).

[22]A. Ashmore, G. Cocconi, A. N. Diddens, and A. M. Wetherell, Phys. Rev. Lett. 5, 576 (1960).

[23]G. Rudstam, Z. Naturforsch. 21A, 1027 (1966).